Identification of Aminopyrimidine-Sulfonamides as Potent Modulators of Wag31-mediated Cell Elongation in Mycobacteria

Vinayak Singh[1*], Neeraj Dhar[2*], János Pató[3], Gaëlle S. Kolly[4], Jana Korduláková[5], Martin Forbak[5], Joanna C. Evans[1], Rita Székely[4], Jan Rybniker[4,12], Zuzana Palčeková[5], Júlia Zemanová[5], Isabella Santi[2], François Signorino-Gelo[2], Liliana Rodrigues[6], Anthony Vocat[4], Adrian S. Covarrubias[7], Monica G. Rengifo[8], Kai Johnsson[8], Sherry Mowbray[7], Joseph Buechler[9], Vincent Delorme[10], Priscille Brodin[10], Graham W. Knott[11], José A. Aínsa[6], Digby F. Warner[1], György Kéri[3†], Katarína Mikušová[5], John D. McKinney[2], Stewart T. Cole[4+], Valerie Mizrahi[1+], Ruben C. Hartkoorn[4,13+*]

[1] MRC/NHLS/UCT Molecular Mycobacteriology Research Unit & DST/NRF Centre of Excellence for Biomedical TB Research, Institute of Infectious Disease and Molecular Medicine & Department of Pathology, University of Cape Town, South Africa

[2] Microbiology and Microsystems, Global Health Institute, Ecole Polytechnique Fédérale de Lausanne, Lausanne, Switzerland

[3] Vichem Chemie Research Ltd., Herman Otto u. 15, 1022 Budapest, Hungary

[4] Microbial Pathogenesis, Global Health Institute, Ecole Polytechnique Fédérale de Lausanne, Lausanne, Switzerland

[5] Comenius University in Bratislava, Faculty of Natural Sciences, Department of Biochemistry, Bratislava, Slovakia

[6] Departamento de Microbiología, Facultad de Medicina, and Instituto de Biocomputación y Física de Sistemas Complejos (BIFI), Universidad de Zaragoza, Zaragoza, Spain

[7] Department of Cell and Molecular Biology, Uppsala University, Biomedical Center, Uppsala, Sweden

[8] Institute of Chemical Sciences and Engineering (ISIC), Ecole Polytechnique Fédérale de Lausanne, Lausanne, Switzerland

[9] Alere (San Diego), Summer Ridge Road, San Diego, CA 92121, USA

[10] Center for Infection and Immunity, Inserm U1019, CNRS UMR8204, Institut Pasteur de Lille, Université de Lille, Lille, France

[11] Interdisciplinary Centre for Electron Microscopy, Ecole Polytechnique Fédérale de Lausanne, Lausanne, Switzerland.

[12] Now at: 1st Department of Internal Medicine, University of Cologne, Cologne, Germany

[13] Now at: Chemical Biology of Antibiotics, Center for Infection and Immunity, Inserm U1019, CNRS UMR8204, Institut Pasteur de Lille, Université de Lille, Lille, France

† Deceased

* These authors contributed equally to this work: co-first author

+ Co-senior author

*Corresponding author: ruben.hartkoorn@inserm.fr

Summary (200 words)

There is an urgent need to discover new anti-tubercular agents with novel mechanisms of action in order to tackle the scourge of drug-resistant tuberculosis. Here, we report the identification of such a molecule – an AminoPYrimidine-Sulfonamide (**APYS1**) that has potent, bactericidal activity against *M. tuberculosis*. Mutations in **APYS1**-resistant *M. tuberculosis* mapped exclusively to *wag31*, a gene that encodes a scaffolding protein thought to orchestrate cell elongation. Recombineering confirmed that a Gln201Arg mutation in Wag31 was sufficient to cause resistance to **APYS1**, however, neither overexpression nor conditional depletion of *wag31* impacted *M. tuberculosis* susceptibility to this compound. In contrast, expression of the wildtype allele of *wag31* in **APYS1**-resistant *M. tuberculosis* was dominant and restored susceptibility to **APYS1** to wildtype levels. Time-lapse imaging and scanning electron microscopy revealed that **APYS1** caused gross malformation of the old pole of *M. tuberculosis*, with eventual lysis. These effects resembled the morphological changes observed following transcriptional silencing of *wag31* in *M. tuberculosis*. These data show that Wag31 is likely not the direct target of **APYS1**, but the striking phenotypic similarity between **APYS1** exposure and genetic depletion of Wag31 in *M. tuberculosis* suggests that **APYS1** might indirectly affect Wag31 through an as yet unknown mechanism.

Introduction

Tuberculosis (TB) is the leading bacterial infection impacted by drug resistance in the world today, with 480,000 cases of multidrug resistant (MDR) TB, comprising 3.6% of all new incident cases of TB, recorded each year (WHO, 2015). In addition to this, extensively drug resistant (XDR) TB has been reported in more than 105 countries (WHO, 2015) and totally drug resistant (TDR) TB (Velayati *et al.*, 2009), for which treatment options are similar to those in the pre-antibiotic era, is becoming increasingly common. Whilst the discovery and introduction of the novel anti-tuberculosis drugs bedaquiline and delamanid are welcome developments and will provide some relief, the fact that anti-tubercular drug discovery and development lags far behind the emergence of drug resistance is indefensible in light of the global burden of this disease. In order to tackle the scourge of drug-resistant TB, it is vital that new antibiotics are discovered that exhibit novel mechanisms of action.

Understanding the mode of action of novel antibiotic molecules serves to aid both the development of new drugs and to establish the vulnerability of targets in *Mycobacterium tuberculosis* against which the compounds act. This field of research is providing a growing picture of new vulnerable and druggable targets in *M. tuberculosis*, including DprEI (first found using benzothiazinones (Makarov *et al.*, 2009)), DnaN (the target of griselimycin (Kling *et al.*, 2015)), ClpC1 (the target of cyclomarin A (Schmitt *et al.*, 2011)), ClpP (the target of cyclic acyldepsipeptides, ADEPs (Ollinger *et al.*, 2012)), cytochrome *bc1* (Q203 (Pethe *et al.*, 2013) and lansoprazol sulfide (Rybniker *et al.*, 2015)) and AtpE (the target of bedaquiline (Andries *et al.*, 2005)).

Here we describe the discovery of a novel anti-TB compound through phenotypic screening of a compound library against replicating *M. tuberculosis*, and the use of next-generation sequencing to demonstrate that resistance is mediated exclusively through mutations in the cell division protein, Wag31. Follow-up experiments using a combination of chemical genetics, time-lapse microscopy and scanning electron microscopy, shed light on the novel, and atypical mechanism of action of this antibiotic.

Results

Aminopyrimidine-sulfonamides (APYS) are potent anti-tubercular compounds

A medium-throughput screen of 15344 small molecules identified a series of three similar AminoPYrimidine-Sulfonamides (**APYS1-3**) with potent activity against replicating *M. tuberculosis* H37Rv, and limited cytotoxicity against a panel of cell lines (Figure 1; Table S1). The most potent of these compounds **(APYS1)** was subsequently shown to be bactericidal with a minimal bactericidal activity (MBC_{99}) of 0.6 µM, similar to its minimal inhibitory concentration (MIC) of 0.3 – 0.6 µM. Further characterisation of these compounds showed that **APYS1-3** did not display any activity against non-replicating *M. tuberculosis*, as determined using the streptomycin-starved 18b model (Sala *et al.*, 2010), suggesting that these compounds target a process essential for cell growth. **APYS1** was also found to be inactive against intracellular H37Rv in both RAW macrophages (up to 20 µM), and in fibroblasts (up to 100 µM). Interestingly, omission of Tween 80 from Middlebrook 7H9 medium significantly impacted the MIC of **APYS1-3** (16-fold increase in MIC_{99}), suggesting that this detergent might facilitate entry of the compound into H37Rv, and providing a possible explanation for the lack of intracellular activity of the compound. All activity data were confirmed with newly synthesised and purified **APYS1-3** compounds (See Supplementary Chemistry for details of chemical synthesis). No significant synergy was observed between **APYS1** and standard anti-tubercular compounds (Table S2). In additional experiments, **APYS1** was also found to be active against *Mycobacterium smegmatis,* albeit only in the presence of an efflux inhibitor (Supplementary Results). As **APYS1** was the most potent of the APYS series, this molecule was taken forward for further investigation into its activity profile and mechanism of action.

Mutations in *wag31* are causal of APYS1 resistance in *M. tuberculosis*

To understand the mechanism of action of **APYS1**, spontaneous **APYS1**-resistant mutants of *M. tuberculosis* H37Rv were isolated independently at two laboratories. Resistant clones were selected on 30 µM **APYS1** (100x MIC) at a frequency of 6×10^{-7}. Eleven individual **APYS1**-resistant clones

(ARC1-11) were picked, grown without **APYS1** and confirmed to be resistant to **APYS1** by the resazurin reduction microplate assay (REMA) (Table 1), whilst not exhibiting cross-resistance to other TB drugs (rifampicin, isoniazid, ethambutol, p-aminosalicylic acid, streptomycin and levofloxacin; data not shown). Whole genome sequence analysis of wildtype H37Rv and three **APYS1**-resistant clones (ARC1-3) revealed that the three resistant clones carried different non-synonymous mutations in *wag31*, which codes for the *M. tuberculosis* "division protein" Wag31 (also known as DivIVA or Ag84). These *wag31* mutations were confirmed by Sanger sequencing. Targeted sequencing of the eight other resistant isolates (ARC4-11) revealed that they all carried non-synonymous mutations at different positions in *wag31* (Table 1). The growth rates of all of the resistant strains in the absence of **APYS1** were indistinguishable from that of the parental *M. tuberculosis* strain (data not shown).

Wag31 is an essential protein in *M. tuberculosis* (Sassetti *et al.*, 2003). It has no known enzymatic activity, but is hypothesised to act as a scaffolding protein that localises to the poles of the bacterium and allows for the proper assembly and function of the elongation machinery (Kang *et al.*, 2008). The more highly conserved N-terminal domain of Wag31 includes the lipid binding domain (LBD) which, in the *Bacillus subtilis* homologue, is important for its polar membrane localisation (van Baarle *et al.*, 2013). In addition, the activity of Wag31 has been shown to be modulated through phosphorylation of threonine 73 (T73) by the Ser/Thr protein kinases, PknA and PknB (Jani *et al.*, 2010). All eleven **APYS1** resistance mutations were, however, located distal to the N-terminus and clustered between Lys190 and Arg213 (Figure 2A and Table 1), strongly implying a fundamental role for this region in the mechanism of resistance, and potentially, in the mechanism of action, of **APYS1** (Figure 2, Table1). Overall, the C-terminal domain of Wag31 is less conserved amongst different species of bacteria, with the resistance-determining region (RDR) being restricted to mycobacteria and close relatives. Interestingly, the residues mutated in **APYS1**-resistant mutants are conserved within the Wag31 homologues of the mycobacterial species analysed (Figure 2). The C-terminal domain is predicted to form a long alpha helix/coil and a helical wheel simulation clustered the

APYS1 mutations mainly on the same side of the helix, which is largely hydrophobic and therefore possibly protected from the aqueous environment by unknown protein-protein interactions.

A Gln201Arg (Q201R) mutation in Wag31 is sufficient to confer resistance of H37Rv to APYS1

To establish whether a single non-synonymous mutation in *wag31* is sufficient to confer resistance of *M. tuberculosis* to **APYS1**, site-directed mutagenesis of the native chromosomal copy of *wag31* was performed by recombineering in H37Rv. A long primer that carried both the non-synonymous mutation (a602g, Q201R) and a synonymous mutation (g609c: to confirm that the Q201R mutation was primer-derived and not the result of spontaneous mutation) was used. **APYS1**-resistant colonies were readily selected and Sanger sequencing confirmed the presence of both mutations in *wag31,* thus corroborating that they arose from recombineering. A selected recombinant colony (H37Rv::Rec-wag31^{Q201R}) was evaluated and found to be resistant to **APYS1** (Table1, MIC_{90} >100 µM), as well as **APYS2** and **APYS3**, while showing unaltered susceptibility to moxifloxacin. Thus, a single non-synonymous mutation in *wag31* is sufficient to cause **APYS1** resistance in *M. tuberculosis*.

Effect of overexpression of *wag31* or *wag31*^{Q201R} on the susceptibility of *M. tuberculosis* to APYS1

To determine the impact of *wag31* overexpression in *M. tuberculosis* on **APYS1** susceptibility, a second copy of either wildtype *wag31* or *wag31*^{Q201R} under control of the native *wag31* promoter, was integrated into both wildtype H37Rv and the **APYS1**-resistant mutant, ARC4. Western blot analysis confirmed that the concentrations of the Wag31 and Wag31^{Q201R} proteins in the recombinant strains were approximately twice that of the control strain (Figure S1). Surprisingly, overexpression of the wildtype allele of *wag31* in H37Rv did not significantly modulate **APYS1** susceptibility (Table 1). In addition, overexpression of *wag31*^{Q201R} in either H37Rv or ARC4 did not impact their susceptibilities to **APYS1** (Table 1). However, expression of wildtype *wag31* in ARC4 restored the **APYS1** susceptibility of this mutant to near wildtype levels (Table 1). These results show that wildtype *wag31* is dominant for the susceptibility of H37Rv to **APYS1**, and expression of

additional mutant or wildtype copies of *wag31* does not significantly modulate activity thus implying that **APYS1** is not a direct inhibitor of Wag31.

Conditional depletion of *wag31* does not affect susceptibility of *M. tuberculosis* to APYS1

Classically, inhibitors of enzymes involved in cellular metabolism become more potent when the cellular concentration of the enzyme is reduced (Evans and Mizrahi, 2015). A similar phenotype may also be expected for a scaffolding protein such as Wag31, although this has not been previously shown. We thus set out to assess the impact of the conditional depletion of Wag31 on the susceptibility of *M. tuberculosis* to **APYS1**. Conditional mutants were constructed by replacing the native *wag31* promoter (*Pwag31*) with a tetracycline (Tet)-regulated promoter (Pmyc1tetO) (Ehrt *et al.*, 2005) (Figure S2), controlled by either the forward Tet repressor (TetR) or reverse Tet repressor (rev-TetR), to produce mutants in the Tet-ON (*wag31* Tet-ON) or Tet-OFF (*wag31* Tet-OFF) configuration, respectively. Both *wag31* Tet-ON and *wag31* Tet-OFF configurations showed ATc dependent growth (Figure 3), confirming the predicted essentiality of *wag31* in *M. tuberculosis* (Sassetti *et al.*, 2003; Griffin *et al.*, 2011), although only the Tet-OFF configuration fully repressed growth and Wag31 protein production (>100 ng/mL of ATc, Figure 3C). ATc had no measurable effect on growth of the parental H37Rv or *wag31*-SCO strains over the concentration range tested.

Potential synergy between Wag31 depletion and **APYS1** activity was investigated using a checkerboard assay on the *M. tuberculosis wag31* Tet-OFF mutant. However, no synergy was observed, even at concentrations of ATc (60-80 ng/mL, Figure 3B) where significant inhibition of growth of the *wag31* Tet-OFF mutant was observed. Synergy was also not seen when *wag31* was silenced 2 days prior to **APYS1** exposure (data not shown). Wag31 depletion therefore did not sensitize *M. tuberculosis* to the toxic effects of **APYS1,** supporting the conclusion that **APYS1** does not directly target Wag31.

APYS1 does not affect mycobacterial cell envelope lipids

Two recent studies showed that acetyl-CoA carboxylases (ACCase) co-localize with, and bind to, Wag31 in *M. smegmatis* (Meniche *et al.*, 2014; Xu *et al.*, 2014). ACCase plays a crucial role in the synthesis of malonyl-CoA, the building block for both fatty acids and mycolic acids in mycobacteria. To investigate whether **APYS1** treatment interferes with Wag31-ACCase interactions, a detailed analysis of fatty acid and mycolic acid production was performed by metabolic labelling (^{14}C-acetate) of lipids in *M. tuberculosis* H37Ra (an avirulent strain that is equally susceptible to **APYS1** as H37Rv; MIC_{90} = 0.25 – 0.5 µM). This analysis revealed that **APYS1** treatment had no effect on the total formation of either fatty acids or mycolic acids (Figure S4). Moreover, **APYS1** had no effecton the total incorporation of ^{14}C-acetate into lipids, however an increase was observed in the extractable lipid compared to cell bound lipids (likely an indirect result of **APYS1** treatment). Additional analyses revealed no major impact of **APYS1** on other prominent cell envelope lipids including trehalose monomycolate (TMM), trehalose dimycolate (TDM), phosphatidylethanolamine (PE), phosphatidylinositol (PI) and phosphatidylinositol mannosides ($acyl_{1\text{-}2}PIM_2$) (Figure S4). Overall, these data suggest that it is unlikely that **APYS1** affects interactions between Wag31 and ACCases.

Single-cell analysis of the effects of APYS1 treatment on *M. tuberculosis*

It has been shown in *M. smegmatis* that the modulation of *wag31* expression has a significant impact on the morphology of the bacterial poles (Nguyen *et al.*, 2007; Kang *et al.*, 2008). Given the evidence implicating Wag31 in the mechanism of resistance of **APYS1**, we evaluated the effect of **APYS1** on *M. tuberculosis* growth and morphology using a microfluidic device coupled to time-lapse microscopy (Wakamoto *et al.*, 2013; Dhar and Manina, 2015). For these experiments, the Erdman strain (another wildtype *M. tuberculosis* strain with the same susceptibility to **APYS1** as H37Rv) was grown initially in **APYS1**-free medium for 3 days, and then exposed to 6 µM **APYS1** for 7 days (between 72-235 h of the time-lapse experiment) before the compound was washed out to allow any survivors to grow. The images revealed that following 24h of **APYS1** exposure, the bacterial poles started to swell and

become globular (Figure 4, Movies S1A and S1B). Swelling was usually restricted to the polar region and, more specifically, to the old growing pole. Whilst the old pole swelled up, bacteria were able to divide once and to generate a daughter cell from their new pole, after which both mother and daughter cells lysed. In support of this, enumerating the bacteria as a function of time following exposure to **APYS1** (Figure S5), showed that the bacterial population nearly doubled, before the cells lysed. Careful examination of the time-lapse microfluidic movies of the polar deformation of H37Rv caused by **APYS1** treatment revealed disproportionate growth of the two lateral walls near the tip, leading to curling and swelling of the polar tips (Figure 4). During the 7 days' exposure to **APYS1**, the majority of the cells lysed and continued to lyse even after washout of the compound. Among the different micro-colonies imaged, approximately 6% had at least one survivor that regrew normally after washout of the compound, and divided to give rise to normal rod-shaped cells. Interestingly, in all of these cases, the survivors originated from the newer-pole sibling.

In supplementary experiments, a similar malformation of the old pole was seen by time-lapse microscopy of *M. smegmatis* in the presence of **APYS1** and the efflux inhibitor verapamil, suggesting a similar mechanism of action of this compound in both mycobacterial species (Movie S3).

Redistribution of Wag31-GFP upon exposure to APYS1

Based on the association between Wag31 mutations and **APYS1** resistance, the impact of **APYS1** on Wag31 polar localization was investigated. To this end, an H37Rv merodiploid strain was constructed by inserting, at the *attB* locus, a copy of *wag31* carrying a 3'-terminal *gfp* fusion (Erdman::*wag31-gfp*) (Santi *et al.*, 2013). Erdman::*wag31-gfp* grew like the parental strain, showed no morphological defects, and was equally susceptible to **APYS1** as the parental Erdman strain (Table 1). Imaging of Erdman::*wag31-gfp* in the GFP channel every 24h (to avoid phototoxicity) showed that, prior to **APYS1** exposure, all cells were normal rod-shaped and showed clear polar and septal localization of Wag31-GFP (Day 0 in Figure 5). As observed for wildtype *M. tuberculosis*, within 24h of exposure to 6

μM **APYS1**, Erdman::*wag31-gfp* started swelling at the poles. In the presence of **APYS1**, Wag31-GFP protein remained localised to the pole, sometimes as a single focal point, and sometimes redistributed into several foci along the edges of the bulbous pole (Figure 5). These data showed that **APYS1** does not affect the overall polar positioning of Wag31 within the cell, but may partially affect the organisation of Wag31 at the pole.

Single-cell analysis of conditional Wag31 depletion in *M. tuberculosis*

To establish whether *M. tuberculosis* has a similar phenotype on Wag31 depletion as previously published in *M. smegmatis* (Kang *et al.*, 2008), and to compare this effect with that of **APYS1** exposure, time-lapse microscopy was carried out on the conditional knockdown mutant, *wag31* Tet-OFF. Bacteria were grown initially in absence of ATc (Movies S2A and S2B) until they formed small microcolonies (3 days), and were subsequently exposed to 2 μg/ml ATc for 7 days (between 75-242 h in the experiment shown in Figure 6). Single-cell analysis showed that bacteria continued to grow and divide normally without any morphological impact for 80-100 h following the addition of ATc. This lag probably reflects the time required to deplete the previously synthesized protein (in agreement with the Western blot analysis shown in Figure 3C). Following this lag however, cells started to swell at their poles, round up and continued to bloat until they burst. Interestingly, and in contrast to **APYS1**-treated bacteria, the newer pole siblings of the ATc-treated *wag31* Tet-OFF mutant were more likely to become globular compared to the older pole sibling, which also swelled but tended to lyse before becoming fully rounded. A small fraction of cells that remained intact during ATc exposure regrew after washout of ATc and gave rise to normal rod-shape daughters.

Electron microscopy of *M. tuberculosis* treated with APYS1

Scanning electron microscopy (SEM) was used to analyse the impact of **APYS1** on H37Rv at high resolution. Whilst control bacteria are classically rod-shaped, exposure of H37Rv to **APYS1** for 24-h led to gross malformation of the polar extremity of the bacilli in a manner similar to that observed in

the time-lapse experiments. From the images shown in Figure 7, it is clear that the swelling of the cell occurs largely away from the septum, at the old pole. In addition, the SEM images clearly confirmed that in cases where a daughter cell had recently separated, it remained rod-shaped (Figure 7B, D and E). The exact shape of the swollen cell pole was variable, with images revealing general polar swelling (Figure 7D), a swollen tight "corkscrew" spiral (Figure 7E), and a swollen open spiral (Figure 7F). Though the exact cause of the different forms of swelling is not understood, these findings are consistent with the microfluidics experiments where different degrees of swelling were observed. The SEM data clearly provide a high-resolution visualisation of the polar deformation of *M. tuberculosis* caused by **APYS1**, and strongly reinforce the role of this compound in disrupting the integrity of the mycobacterial cell wall.

Discussion

Tuberculosis is a global health problem, and the bacterial infection most impacted by multidrug resistance. It is therefore essential to discover new classes of antibiotic, and to gain insight into their underlying mechanisms of action in order to identify and exploit new vulnerabilities in *M. tuberculosis*. Here, we report the discovery of a novel anti-tubercular, **APYS1**, and utilise a combination of genetic and microscopy techniques to investigate its mechanism of action.

Elucidating the mechanism by which a susceptible bacterium becomes resistant to an antibiotic is a powerful means of gaining insight into its mode of action. Generally, resistance mutations are either associated with the antibiotic target itself; linked to a mechanism by which the bacterium can eliminate or detoxify the antibiotic, largely through increased antibiotic efflux or metabolic inactivation; or, in the case of a prodrug, located in a gene(s) involved in its metabolic activation. Our data clearly show that single point mutations clustered within a region of *wag31* can render *M. tuberculosis* resistant to the anti-tubercular activity of **APYS1**. However, overexpression of a second copy of either the mutant or wildtype *wag31* allele in wildtype *M. tuberculosis* did not impact **APYS1** susceptibility. Moreover, transcriptional silencing of *wag31* transcription in *M. tuberculosis* did not synergise with the activity of **APYS1**. These findings suggest that while *wag31* is clearly involved in the mechanism of resistance to **APYS1**, Wag31 itself is not the direct target of **APYS1**.However, a pivotal observation was that expression of wildtype *wag31* in a resistant isolate of H37Rv (ARC4, carrying a Gln201Arg mutation in *wag31*), was dominant, and reverted the **APYS1**-resistant phenotype of ARC4 to susceptible (i.e., complemented resistance). This indicates that the presence of a wildtype *wag31* allele is sufficient for **APYS1** activity, even though this activity cannot be modulated by decreasing or increasing *wag31* expression in wildtype H37Rv. To our knowledge, this phenotype has not been observed previously with any chemical compounds in bacteria, and clearly suggests an atypical and novel mechanism of action. A possible explanation is that APYS1 binds another protein and that this complex (APYS1-protein X) interacts with wildtype Wag31, causing cell

death. The resistance mutations in Wag31 would prevent the binding of APYS1-protein X and therefore prevent cell death. However, it remains unclear as to why such an interaction cannot be titrated.

Wag31 is a scaffolding protein that binds to the negative curvature of the polar cell wall (Lenarcic *et al.*, 2009; Ramamurthi and Losick, 2009; Oliva *et al.*, 2010), and allows for the correct placement and coordination of partner proteins for elongation and the biosynthesis of cell wall precursors (Nguyen *et al.*, 2007; Meniche *et al.*, 2014). In *M. tuberculosis*, Wag31, is present exclusively at growing poles, and is recruited to the new pole only after the septum has been formed (Santi *et al.*, 2013). Previous work has demonstrated that conditional depletion of *wag31* was associated with the swelling and deformation of the bacterial pole in *M. smegmatis* (Kang *et al.*, 2008). Time-lapse microscopy of single cells clearly demonstrated that conditional depletion of Wag31 in *M. tuberculosis* had a very similar effect, with this imaging modality revealing swelling/bulging of the bacterial "new" pole and eventual bacterial lysis. Interestingly, exposure of *M. tuberculosis* and *M. smegmatis* to **APYS1** also resulted in a very clear and similar swelling/bulging of the bacterial pole, however, in this case, it was primarily the "old" pole that was affected. The differential polar deformation between Wag31 depletion and **APYS1** exposure is likely due to differences in the effects of conditional protein depletion *versus* compound activity. Specifically, arrest of *de novo* production of Wag31 by transcriptional silencing of *wag31* would have little impact on the old pole where Wag31 is already present, but would primarily impact the new pole to which Wag31 is recruited after septum formation. In contrast, perturbation of Wag31 or its associated function by a compound such as **APYS1** is likely to act where Wag31 is already active, and hence, demonstrate a preference for the older, elongating pole. Visualisation of the distribution of Wag31-GFP showed that Wag31 remained localised at the poles following the addition of **APYS1**, although in some cases there was a redistribution of the protein at the old pole. Moreover, instead of swelling evenly, some of the poles continued to elongate along one side causing the tips to curl – a phenotype perhaps associated with

the localisation of Wag31 and confirmed in SEM images. Although the genetic studies argued against Wag31 being the direct target of **APYS1**, time-lapse microscopy showed significant morphological similarities between **APYS1** treatment and Wag31 depletion, suggesting that Wag31 may play an important role in the mechanism of action of **APYS1**, albeit not as the direct target.

Conditional depletion of Wag31 is likely to lead to inadequate scaffolding and orchestration of cell elongation, potentially through the inability to co-ordinate the positioning of partner proteins, leading to weakening of the cell wall and polar bulging. Given the role of *wag31* mutations in conferring resistance to **APYS1**, and the similar effects of Wag31 depletion and **APYS1** treatment on mycobacterial morphology, one could postulate that **APYS1** acts by affecting the binding of one or more partner proteins to Wag31. This hypothesis is supported by the spatial clustering of the **APYS1** resistance mutations on one hydrophobic flank of the Wag31 helix, suggestive of a site for protein-protein interactions. Wag31 has been reported to interact with proteins of the ACCase complex involved in cell envelope lipid formation (Meniche *et al.*, 2014), the protein kinase, PknB (Kang *et al.*, 2005; Kang *et al.*, 2008), and a small uncharacterised Mycobacterium-specific protein, CwsA (Plocinski *et al.*, 2012; Plocinski *et al.*, 2013). Our analysis of cell envelope lipids showed that it is unlikely that **APYS1** affects an interaction with the ACCase complex. Interestingly, however, conditional depletion or overexpression of PknB has been shown to cause swelling of *M. smegmatis* (Kang *et al.*, 2005; Kang *et al.*, 2008; Chawla *et al.*, 2014), and overexpression of CwsA likewise resulted in polar swelling in both *E. coli* and *M. smegmatis* through an unknown mechanism (Plocinski *et al.*, 2013). Thus, **APYS1** may act to perturb Wag31::PknB or Wag31::CwsA interactions, although it is unclear as to why these interactions cannot be titrated by depletion or overexpression of Wag31. It is worth noting that **APYS1** shares a similar chemical scaffold to navitoclax, a largely linear molecule with a 4-aminobenzene-1-sulfonamidecore, that is an effective inhibitor of protein-protein interactions between the human apoptosis regulatory protein, BCL-2, and its pro-apoptotic partner, BAX (Souers *et al.*, 2013; Arkin *et al.*, 2014).

Alternatively, **APYS1** might affect *M. tuberculosis* through an as yet undefined mechanism associated with Wag31. As an example, the bulging of the mycobacterial cell pole is reminiscent of deformations observed following weakening of the peptidoglycan component of the cell wall by the β-lactam antibiotic, meropenem (Chao *et al.*, 2013); by conditional depletion of the penicillin binding protein, PonA (Kieser *et al.*, 2015); or by overexpression of the active form of the peptidoglycan hydrolase, RipA (Chao *et al.*, 2013). Wag31 has previously been suggested to co-ordinate peptidoglycan synthesis (Nguyen *et al.*, 2007; Kang *et al.*, 2008), and a recent report showed that in *M. smegmatis* Wag31 was enriched in the fraction containing plasma membrane tightly associated to the cell wall fraction (PM-CW) rather than the pure plasma membrane fraction (PMf) (Hayashi *et al.*, 2016), which hints at the possibility of Wag31 to interact directly with periplasmic proteins involved in peptidoglycan biosynthesis. Future studies that build upon on these observations, are likely to shed light on the exact mechanism through which **APYS1** acts.

Experimental Procedures:

Isolation of H37Rv resistant mutants to APYS1

Spontaneous mutants of H37Rv resistant to **APYS1** were isolated in parallel at two different research sites. Briefly wildtype H37Rv (10^8 or 10^9 CFU) was plated on Middlebrook 7H10 or 7H11 agar supplemented with 0.5 % glycerol and 10% OADC, and containing **APYS1** (10x, 20x, 50x and 100x MIC). Following incubation (4 weeks, 37˚C), colonies were selected and sub-cultured in Middlebrook 7H9 broth (supplemented with 0.2 % glycerol, 0.05% Tween 80 and 10% ADC). Selected isolates were screened for their susceptibility to **APYS1** as well as rifampicin, isoniazid, ethambutol, p-aminosalicylic acid, streptomycin and levofloxacin. The parental H37Rv strain and three resistant isolates with confirmed resistance to **APYS1** were subjected to whole-genome sequencing on Illumina HiSEQ sequencer (as per manufacture's protocol), and single nucleotide polymorphisms identified using HTStation (David *et al.*, 2014). Mutations identified in *wag31* (*Rv2145c/divIVA*) were confirmed by Sanger sequencing, and tested in the remaining 8 resistant isolates that did not undergo whole genome sequencing (Primers Wag31 seq F and Wag31 seq R, Table S3).

Construction of H37Rv and ARC4 carrying a second copy of *wag31* or *wag31*^{Q201R}

Wild type *wag31* and *wag31*$^{Q201)}$ with the native promoter (149 bp 5'-terminal to the start codon of *wag31*) were PCR amplified using the primers listed in Table S3, from parental H37Rv and **APYS1**-resistant ARC4. The amplified product was digested with *EcoRI* and cloned into the integrative shuttle plasmid pTT1B::Gm (Abrahams *et al.*, 2012) to generate pTTwag31 and pTTwag31$^{(Q201R)}$ respectively. Control plasmid pTT1B, pTTwag31 and pTTwag31$^{(Q201R)}$ were electroporated into H37Rv and ARC4 to produce H37Rv::pTT1B, H37Rv::pTTwag31, H37Rv::pTTwag31$^{(Q201R)}$, ARC4::pTT1B, ARC4::pTTwag31 and ARC4::pTTwag31^{Q201R} respectively. The susceptibility of these strains to **APYS1** was then determined by REMA.

Time-lapse microscopy

Time-lapse microscopy of wildtype *M. tuberculosis* (Erdman), the *M. tuberculosis* strain expressing Wag31-GFP (Erdman::*wag31-gfp*) and *wag31* Tet-OFF was carried out as described previously (Dhar and Manina, 2015). Bacterial cultures were grown to mid-exponential phase ($A_{600\ nm}$ = 0.5) and concentrated ten-fold by centrifugation. Bacterial clumps were excluded by filtering through a 5 μm filter and the suspension comprising predominantly of single cells were assembled in a microfluidic device. Imaging of the bacteria was carried out using a 100x oil-immersion phase objective (Olympus Plan Semi Apochromat, 1.3 NA) on a Deltavision PersonalDV inverted microscope (GE Healthcare) fitted with an environmental chamber set at 37^0C. Fresh 7H9 medium (supplemented with either 3 μg/ml **APYS1**, during the drug exposure period or 2 μg/ml anhydrotetracycline for conditional depletion of Wag31 in the *wag31* Tet-OFF strain was pumped through the device at a flow-rate of 15 μl/min using a syringe pump. Imaging was carried out at 30 min or 60 min intervals in case of *wag31* Tet-OFF and H37Rv, respectively, on the phase channel. In case of the *M. tuberculosis* strain expressing Wag31-GFP, images were captured once every 24h, on the phase and FITC channels (Excitation filter 490/20, Emission filter 528/38). About 50-70 distinct positions in the microfluidic device were imaged in a typical experiment. Images were processed and movies assembled using Softworx 4.1 (Applied Precision, GE Healthcare) or ImageJ v 1.47n (Rasband, 2015).

Additional methods and details of the chemical syntheses of **APYS1-3** are described in the Supplementary Methods section.

Author contributions

Conceptualization: V.S., N.D., G.K., S.T.C., V.M. and R.C.H. Investigation: V.S., N.D., J.P., G.S.K., J.K., M.F., J.C.E., R.S., J.R, Z.P., J.Z., I.S., F.S-G, L.R., A.V., A.S.C, M.S.R., V.D., K.M. and R.C.H. Resources: J.B. Supervision: K.J., S.M., P.B., G.W.K., J.A.A., D.F.W., G.K., K.M., J.D.M., S.T.C., V.M., R.C.H. Writing – Original Draft: V.S., N.D., J.P., K.M., S.T.C., V.M., R.C.H. Project Administration: S.T.C., V.M. and R.C.H.

Acknowledgements

This work was funded by the European Community's Seventh Framework Programme (Grant 260872); the South African Medical Research Council (to V.M.); the National Research Foundation of South Africa (to V.M.); a Senior International Research Scholar's grant from the HHMI (Grant 55007649 to V.M.); the Bill & Melinda Gates Foundation (HIT-TB sub-award to V.M. from the FNIH), the European Commission Marie Curie Fellowship (PIEF-GA-2012-327219 to R.S.) and the Slovak Research and Development Agency (Contract No. DO7RP-0015-11 to K.M.). We dedicate this work to the late Dr. György Kéri, an avid supporter of anti-tuberculosis research.

R.C.H., S.T.C., J.P. and G.K. are named inventors on patents relating to this work

References

Abrahams, G.L., Kumar, A., Savvi, S., Hung, A.W., Wen, S., Abell, C., *et al.* (2012) Pathway-selective sensitization of mycobacterium tuberculosis for target-based whole-cell screening. *Chem Biol* **19**: 844–854.

Andries, K., Verhasselt, P., Guillemont, J., Gohlmann, H.W., Neefs, J.M., Winkler, H., *et al.* (2005) A diarylquinoline drug active on the ATP synthase of Mycobacterium tuberculosis. *Science (80-)* **307**: 223–227.

Arkin, M.R., Tang, Y., and Wells, J.A. (2014) Review Small-Molecule Inhibitors of Protein-Protein Interactions : Progressing toward the Reality. *Chem Biol* **21**: 1102–1114 http://dx.doi.org/10.1016/j.chembiol.2014.09.001.

Baarle, S. van, Celik, I.N., Kaval, K.G., Bramkamp, M., Hamoen, L.W., and Halbedel, S. (2013) Protein-Protein Interaction Domains of Bacillus subtilis DivIVA. *J Bacteriol* **195**: 1012–1021 http://jb.asm.org/cgi/doi/10.1128/JB.02171-12.

Chao, M.C., Kieser, K.J., Minami, S., Mavrici, D., Aldridge, B.B., Fortune, S.M., *et al.* (2013) Protein Complexes and Proteolytic Activation of the Cell Wall Hydrolase RipA Regulate Septal Resolution in Mycobacteria. **9**.

Chawla, Y., Upadhyay, S., Khan, S., Nagarajan, S.N., Forti, F., and Nandicoori, V.K. (2014) Protein Kinase B (PknB) of Mycobacterium tuberculosis Is Essential for Growth of the Pathogen in Vitro as well as for Survival within the Host *. **289**: 13858–13875.

David, F.P.A., Delafontaine, J., Carat, S., Ross, F.J., Lefebvre, G., Jarosz, Y., *et al.* (2014) HTSstation: A web application and open-access libraries for high-throughput sequencing data analysis. *PLoS One* **9**.

Dhar, N., and Manina, G. (2015) Single-cell analysis of mycobacteria using microfluidics and time-lapse microscopy. *Methods Mol Biol* **1285**: 241–56 http://www.ncbi.nlm.nih.gov/pubmed/25779320. Accessed February 12, 2016.

Ehrt, S., Guo, X. V, Hickey, C.M., Ryou, M., Monteleone, M., Riley, L.W., and Schnappinger, D. (2005)

Controlling gene expression in mycobacteria with anhydrotetracycline and Tet repressor. *Nucleic Acids Res* **33**: e21 http://www.pubmedcentral.nih.gov/articlerender.fcgi?artid=548372&tool=pmcentrez&rendertype=abstract.

Evans, J.C., and Mizrahi, V. (2015) The application of tetracyclineregulated gene expression systems in the validation of novel drug targets in Mycobacterium tuberculosis. *Front Microbiol* **6**: 1–14.

Griffin, J.E., Gawronski, J.D., DeJesus, M.A., Ioerger, T.R., Akerley, B.J., and Sassetti, C.M. (2011) High-resolution phenotypic profiling defines genes essential for mycobacterial growth and cholesterol catabolism. *PLoS Pathog* **7**.

Hayashi, J.M., Luo, C.-Y., Mayfield, J.A., Hsu, T., Fukuda, T., Walfield, A.L., *et al.* (2016) Spatially distinct and metabolically active membrane domain in mycobacteria. *Proc Nat Acad Sci U S A* **113**: 201525165 http://www.pnas.org/content/early/2016/04/21/1525165113.abstract\nhttp://www.pnas.org/lookup/doi/10.1073/pnas.1525165113.

Jani, C., Eoh, H., Lee, J., Hamasha, K., Sahana, M., Han, J.-S., *et al.* (2010) Regulation of Polar Peptidoglycan Biosynthesis by Wag31 Phosphorylation in Mycobacteria. *BMC Microbiol* **10**: 327 http://www.biomedcentral.com/1471-2180/10/327.

Kang, C.M., Abbott, D.W., Sang, T.P., Dascher, C.C., Cantley, L.C., and Husson, R.N. (2005) The Mycobacterium tuberculosis serine/threonine kinases PknA and PknB: Substrate identification and regulation of cell shape. *Genes Dev* **19**: 1692–1704.

Kang, C.-M., Nyayapathy, S., Lee, J.-Y., Suh, J.-W., and Husson, R.N. (2008) Wag31, a homologue of the cell division protein DivIVA, regulates growth, morphology and polar cell wall synthesis in mycobacteria. *Microbiology* **154**: 725–735 http://mic.microbiologyresearch.org/content/journal/micro/10.1099/mic.0.2007/014076-0.

Kieser, K.J., Boutte, C.C., Kester, J.C., Baer, C.E., Barczak, A.K., Meniche, X., *et al.* (2015) Phosphorylation of the Peptidoglycan Synthase PonA1 Governs the Rate of Polar Elongation in

Mycobacteria. *PLOS Pathog* **11**: e1005010 http://dx.plos.org/10.1371/journal.ppat.1005010.

Kling, A., Lukat, P., Almeida, D. V., Bauer, A., Fontaine, E., Sordello, S., *et al.* (2015) Targeting DnaN for tuberculosis therapy using novel griselimycins. *Science (80-)* **348**: 1106–1112.

Lenarcic, R., Halbedel, S., Visser, L., Shaw, M., Wu, L.J., Errington, J., *et al.* (2009) Localisation of DivIVA by targeting to negatively curved membranes. *EMBO J* **28**: 2272–82.

Makarov, V., Manina, G., Mikusova, K., Möllmann, U., Ryabova, O., Saint-Joanis, B., *et al.* (2009) Benzothiazinones kill Mycobacterium tuberculosis by blocking arabinan synthesis. *Science* **324**: 801–4.

Meniche, X., Otten, R., Siegrist, M.S., Baer, C.E., Murphy, K.C., Bertozzi, C.R., and Sassetti, C.M. (2014) Subpolar addition of new cell wall is directed by DivIVA in mycobacteria. *Proc Natl Acad Sci U S A* **111**: E3243-51 http://www.pnas.org/content/111/31/E3243.full.

Nguyen, L., Scherr, N., Gatfield, J., Walburger, A., Pieters, J., and Thompson, C.J. (2007) Antigen 84, an effector of pleiomorphism in Mycobacterium smegmatis. *J Bacteriol* **189**: 7896–910 http://www.ncbi.nlm.nih.gov/pubmed/17766411.

Oliva, M. a, Halbedel, S., Freund, S.M., Dutow, P., Leonard, T. a, Veprintsev, D.B., *et al.* (2010) Features critical for membrane binding revealed by DivIVA crystal structure. *EMBO J* **29**: 1988–2001.

Ollinger, J., O'malley, T., Kesicki, E.A., Odingo, J., and Parish, T. (2012) Validation of the essential ClpP protease in Mycobacterium tuberculosis as a novel drug target. *J Bacteriol* **194**: 663–668.

Pethe, K., Bifani, P., Jang, J., Kang, S., Park, S., Ahn, S., *et al.* (2013) Discovery of Q203, a potent clinical candidate for the treatment of tuberculosis. *Nat Med* **19**: 1157–60 http://www.ncbi.nlm.nih.gov/pubmed/23913123.

Plocinski, P., Arora, N., Sarva, K., Blaszczyk, E., Qin, H., Das, N., *et al.* (2012) Mycobacterium tuberculosis CwsA interacts with CrgA and Wag31, and the CrgA-CwsA complex is involved in peptidoglycan synthesis and cell shape determination. *J Bacteriol* **194**: 6398–6409.

Plocinski, P., Martinez, L., Sarva, K., Plocinska, R., Madiraju, M., and Rajagopalan, M. (2013)

Mycobacterium tuberculosis CwsA overproduction modulates cell division and cell wall synthesis. *Tuberculosis* **93**: S21–S27 http://linkinghub.elsevier.com/retrieve/pii/S1472979213700064.

Ramamurthi, K.S., and Losick, R. (2009) Negative membrane curvature as a cue for subcellular localization of a bacterial protein. *Proc Natl Acad Sci U S A* **106**: 13541–13545.

Rasband, W. (2015) ImageJ. *U S Natl Institutes Heal Bethesda, Maryland, USA* //imagej.nih.gov/ij/.

Rybniker, J., Vocat, A., Sala, C., Busso, P., Pojer, F., Benjak, A., and Cole, S.T. (2015) Lansoprazole is an antituberculous prodrug targeting cytochrome bc1. *Nat Commun* **6**: 7659.

Sala, C., Dhar, N., Hartkoorn, R.C., Zhang, M., Ha, Y.H., Schneider, P., and Cole, S.T. (2010) Simple model for testing drugs against nonreplicating Mycobacterium tuberculosis. *Antimicrob Agents Chemother* **54**: 4150–4158.

Santi, I., Dhar, N., Bousbaine, D., Wakamoto, Y., and McKinney, J.D. (2013) Single-cell dynamics of the chromosome replication and cell division cycles in mycobacteria. *Nat Commun* **4**: 2470.

Sassetti, C.M., Boyd, D.H., and Rubin, E.J. (2003) Genes required for mycobacterial growth defined by high density mutagenesis. *Mol Microbiol* **48**: 77–84.

Schmitt, E.K., Riwanto, M., Sambandamurthy, V., Roggo, S., Miault, C., Zwingelstein, C., *et al.* (2011) The natural product cyclomarin kills mycobacterium tuberculosis by targeting the ClpC1 subunit of the caseinolytic protease. *Angew Chemie - Int Ed* **50**: 5889–5891.

Souers, A.J., Leverson, J.D., Boghaert, E.R., Ackler, S.L., Catron, N.D., Chen, J., *et al.* (2013) ABT-199 , a potent and selective BCL-2 inhibitor , achieves antitumor activity while sparing platelets. *Nat Med* **19**: 202–208 http://dx.doi.org/10.1038/nm.3048.

Velayati, A.A., Masjedi, M.R., Farnia, P., Tabarsi, P., Ghanavi, J., ZiaZarifi, A.H., and Hoffner, S.E. (2009) Emergence of new forms of totally drug-resistant tuberculosis bacilli: Super extensively drug-resistant tuberculosis or totally drug-resistant strains in Iran. *Chest* **136**: 420–425.

Wakamoto, Y., Dhar, N., Chait, R., Schneider, K., Signorino-Gelo, F., Leibler, S., and McKinney, J.D. (2013) Dynamic Persistence of Antibiotic-Stressed Mycobacteria. *Science (80-)* **339**: 91–95 http://www.sciencemag.org/cgi/doi/10.1126/science.1229858\nhttp://www.sciencemag.org/con

tent/339/6115/91\nhttp://www.sciencemag.org/content/339/6115/91.full.pdf.

WHO (2015) Global Tuberculosis Report 2015. http://www.ncbi.nlm.nih.gov/pubmed/15003161.

Xu, W.X., Zhang, L., Mai, J.T., Peng, R.C., Yang, E.Z., Peng, C., and Wang, H.H. (2014) The Wag31 protein interacts with AccA3 and coordinates cell wall lipid permeability and lipophilic drug resistance in Mycobacterium smegmatis. *Biochem Biophys Res Commun* **448**: 255–260 http://dx.doi.org/10.1016/j.bbrc.2014.04.116.

Table 1. Summary of **APYS1** susceptibility of different *M. tuberculosis* clones and constructs, and their *wag31* genotype.

Strain/Isolate	MIC (µM)	Base mutation in *wag31*	Amino acid substitution in Wag31
H37Rv	0.3-0.6	WT	WT
ARC1	6.25-12.5	c637g	R213G
ARC2	6.25-12.5	c601a	Q201K
ARC3	6.25-12.5	c637t	R213C
ARC4	100	a602g	Q201R
ARC5	50-100	g570c	K190N
ARC6	25	g570t	K190N
ARC7	6.25-12.5	g638t	R213L
ARC8	25-50	g570t	K190N
ARC9	25-50	g570t	K190N
ARC10	25-50	c625t	L209F
ARC11	12.5-25	c622t	R208G
H37Rv::Rec-wag31^{Q201R}	>100	a602g	Q201R
H37Rv:: pTT1B (control)	0.2-0.5	WT	WT
H37Rv:: pTTwag31	0.2-0.5	WT + WT	WT + WT
H37Rv:: pTTwag31^{Q201R}	0.2-0.5	WT + a602g	WT + Q201R
ARC4:: pTT1B (control)	100	a602g	Q201R
ARC4:: pTTwag31	1.56	a602g + WT	Q201R + WT
ARC4:: pTTwag31 ^{Q201R}	100	a602g + a602g	Q201R + Q201R
Erdman	0.3-0.6	WT	WT
Erdman::*wag31-gfp*	0.3-0.6	WT + WT-gfp	WT + WT-gfp
H37Ra	0.25-0.5	WT	WT

Figure Legends

Figure 1: Structures of the anti-tubercular aminopyrimidine-sulfonamides identified by phenotypic screening

Figure 2: (A) A model summarising the multiple protein alignment of Wag31 from various rod-shaped bacteria (not Gram negative). There are three main conserved regions (CR1-3) (numbering for *M. tuberculosis* and *B. subtilis* indicated). The resistance determining region (RDR) shows the region where mutations were found in *M. tuberculosis wag31* that confer resistance to **APYS1**, a region not found in the *B. subtilis* homolog. Threonine 73 (T73) represents the site of phosphorylation of *M. tuberculosis* Wag31. (B) The bases and amino acids in the RDR of *wag31* (both in red) that were mutated in the eleven **APYS1**-resistant strains. (C) A multiple alignment of the RDR in a number of rod-shaped bacteria shows that this region is largely conserved in mycobacteria, carries multiple mutations in *C. glutamicum* and is mostly absent from other rod-shaped Gram-positive bacteria. Red asterisks represent the amino acids found to be mutated in **APYS1**-resistant *M. tuberculosis*. (D) A helical wheel representation of the RDR of Wag31 (amino acid 184-219) shows that the mutated residues (with dark edge) are located primarily on one side of the wheel (http://rzlab.ucr.edu/scripts/wheel).

Figure 3: (A) The impact of conditional transcription repression of *wag31* on the relative growth rate of *wag31* Tet-OFF (open squares) and *wag31* Tet-ON (black circles) as a function of the concentration of ATc in the culture medium. Data are the mean and SD of triplicate samples (see also Figure S3). (B) The 7-day **APYS1** susceptibility of *wag31* Tet-OFF grown in the absence (black circles) and presence of ATc (open circles [60 ng/ml]; open square [70 ng/mL]; open triangle [80 ng/mL]; and open diamond [100 ng/mL]). The data show that the ability to inhibit bacterial growth by **APYS1** is not impacted by ATc-mediated silencing of *wag31* expression. (C) Western blot analysis of ATc-

dependent and time-dependent depletion of Wag31 in *wag31* Tet-OFF. Strains were cultured in Middlebrook 7H9 broth and either left untreated (-) or exposed to ATc (500 ng/mL) (+) for the indicated length of time. Western Blots were probed with anti-Wag31 antibodies and anti-ThyX antibodies (loading control).

Figure 4: Single-cell analysis of the effect of APYS1 on *M. tuberculosis*. Bacteria were cultured in a microfluidic device and imaged at 1 h intervals on the phase channel. Bacteria were exposed to 6 µM of **APYS1** compound between 72-235 h. The images shown depict representative time-series snapshots of two positions in the microfluidic device that were imaged. Typically, in a time-lapse microscopy experiment, approximately 50-70 points are imaged. The white horizontal bar represents 5 µm. The arrows point to swollen, polar regions of cells, whereas the arrowheads point to cells in which one side of the bacterium seems to elongate more than the opposite side, causing the tips to curl inwards.

Figure 5: Exposure to APYS1 causes partial redistribution of Wag31-GFP in *M. tuberculosis*. Cells expressing Wag31-GFP were exposed to 6 µM **APYS1** and imaged on day 0 (D0) and after 1, 2, 3 and 5 days after exposure. Representative time-series snapshots of bacteria are shown. The red color represents the phase channel and the green channel represents the FITC channel (Wag31-GFP). On exposure to **APYS1**, the Wag31-GFP signal, which is usually a defined focus at the poles, becomes redistributed and spreads out at the poles followed by swelling of the poles (white arrows). The horizontal scale bar represents 3 µm.

Figure 6: Single-cell analysis of effect of transcriptional silencing of *wag31* in *M. tuberculosis*. *wag31* Tet-OFF bacteria were grown in a microfluidic device and imaged at 30 min intervals on the phase channel. To knockdown the expression of Wag31 protein, the bacteria were exposed to 2

µg/ml ATc between 75-242 h. After a lag of 80-100 h, cells started to lyse and some of the new-pole siblings began to swell and become globular (white arrows). The images shown are representative time-series snapshots of two positions in the microfluidic device that were imaged. The white horizontal scale bar represents 5 µm.

Figure 7. Scanning electron microscopy (SEM) images of **(A and C)** H37Rv in the absence of **APYS1** and **(B, D, E, and F)** H37Rv following 24 hrs of 3 µM **APYS1** exposure. The images show a variety of polar deformations due to the compound. The white scale bar represents 1 µm.

Table Legends

Table 1. APYS1 susceptibility of different *M. tuberculosis* strains with altered *wag31* genotypes.

Figure 1:

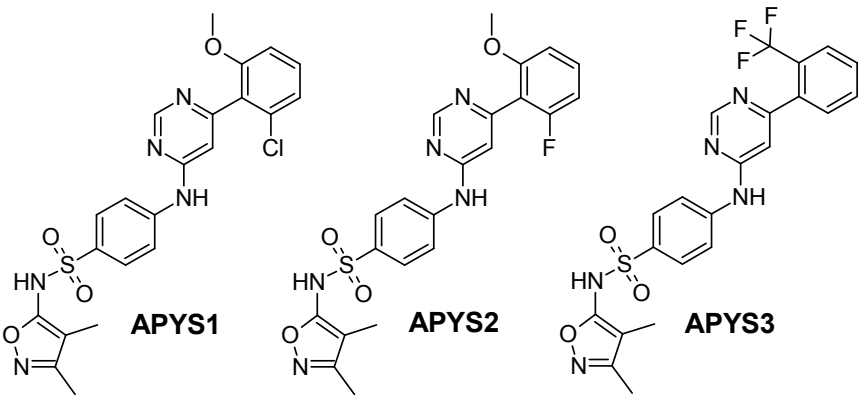

Figure 2:

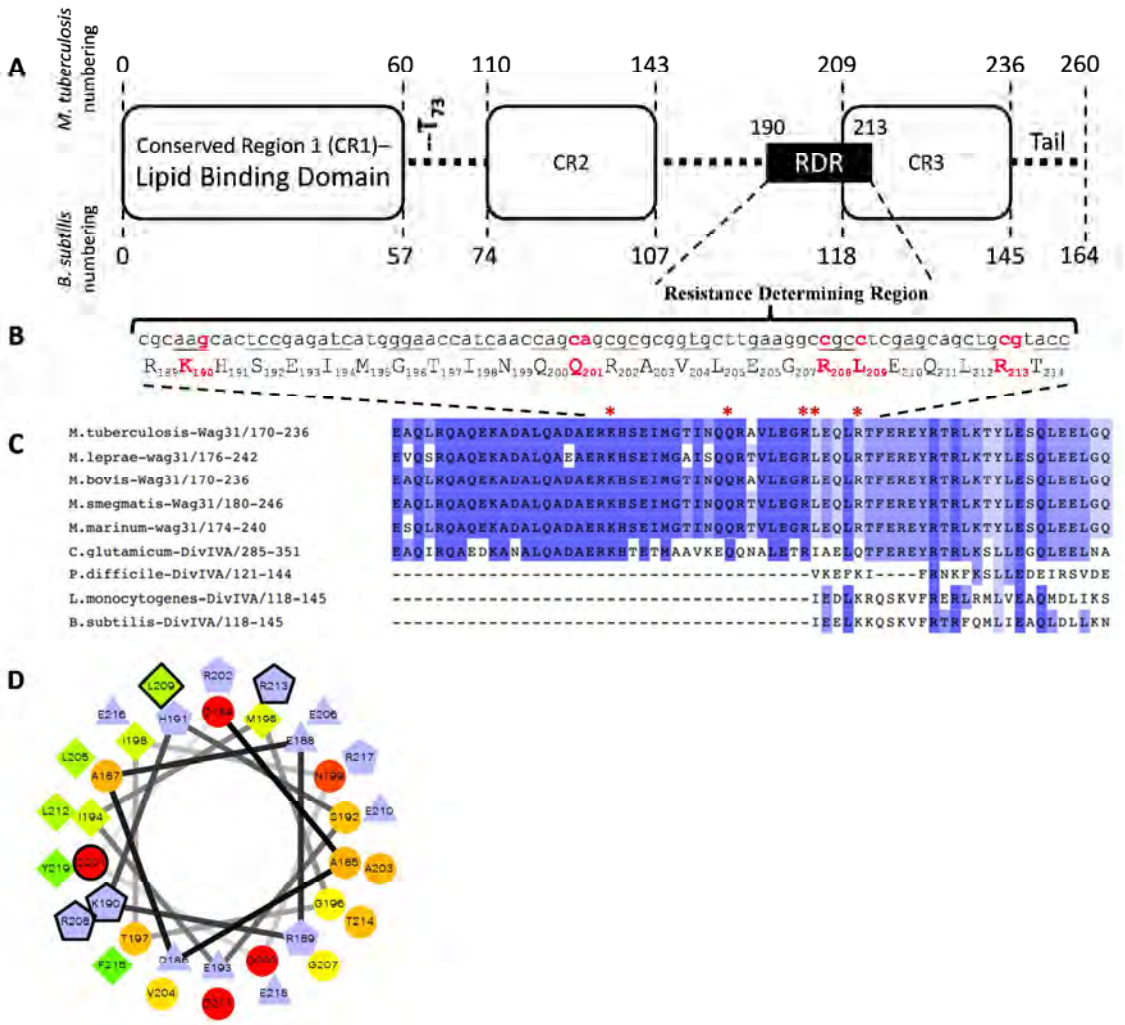

Hydrophilic residues: circles (most hydrophilic (uncharged) residue in red, decreasing proportionally to the hydrophilicity), hydrophobic residues: diamonds (most hydrophobic residue is green, decreasing proportionally to the hydrophobicity). Zero hydrophobicity coded as yellow. The potentially charged residues are light blue.

Figure 3:

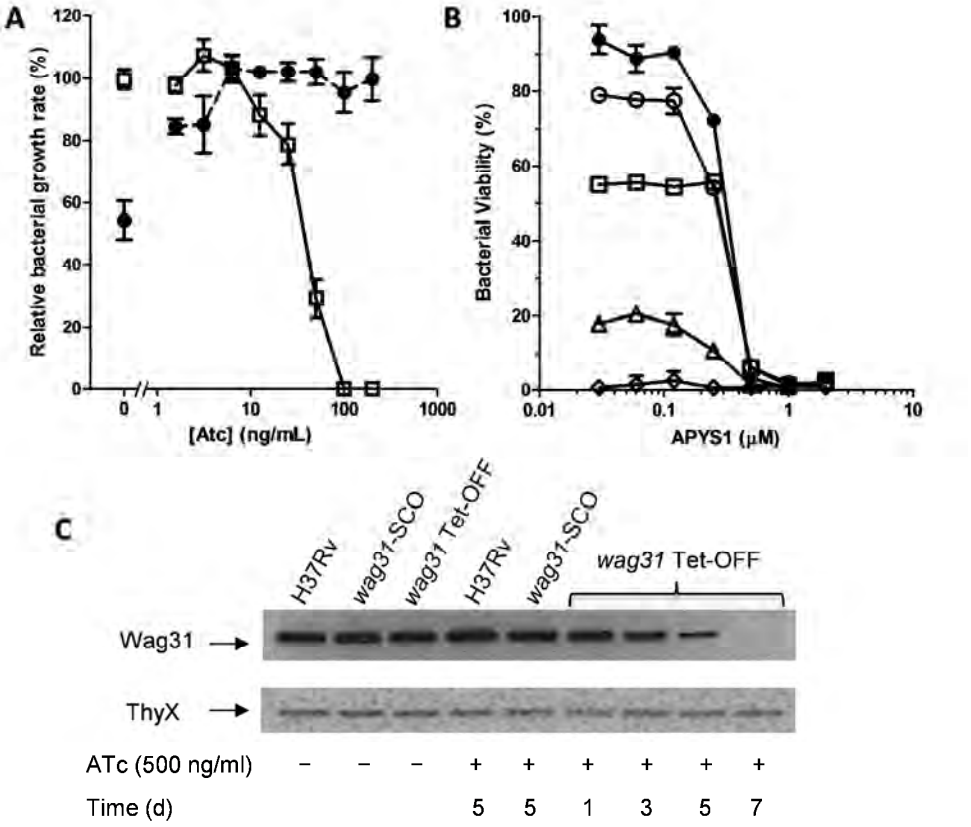

Figure 4:

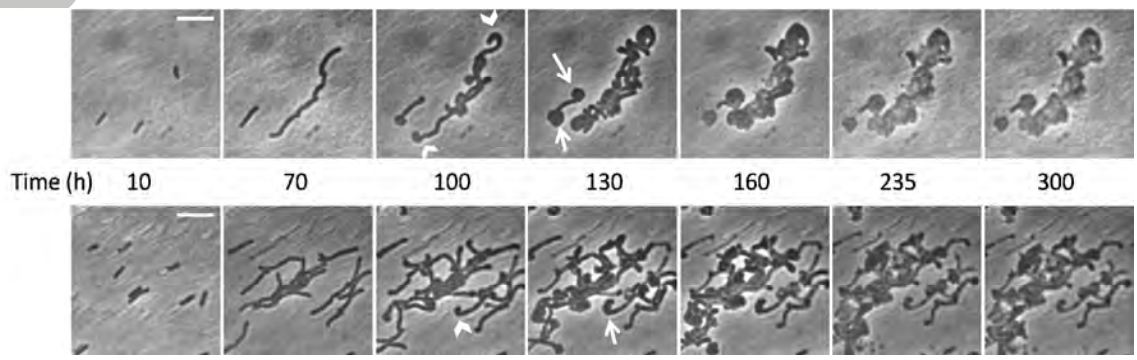

Figure 5:

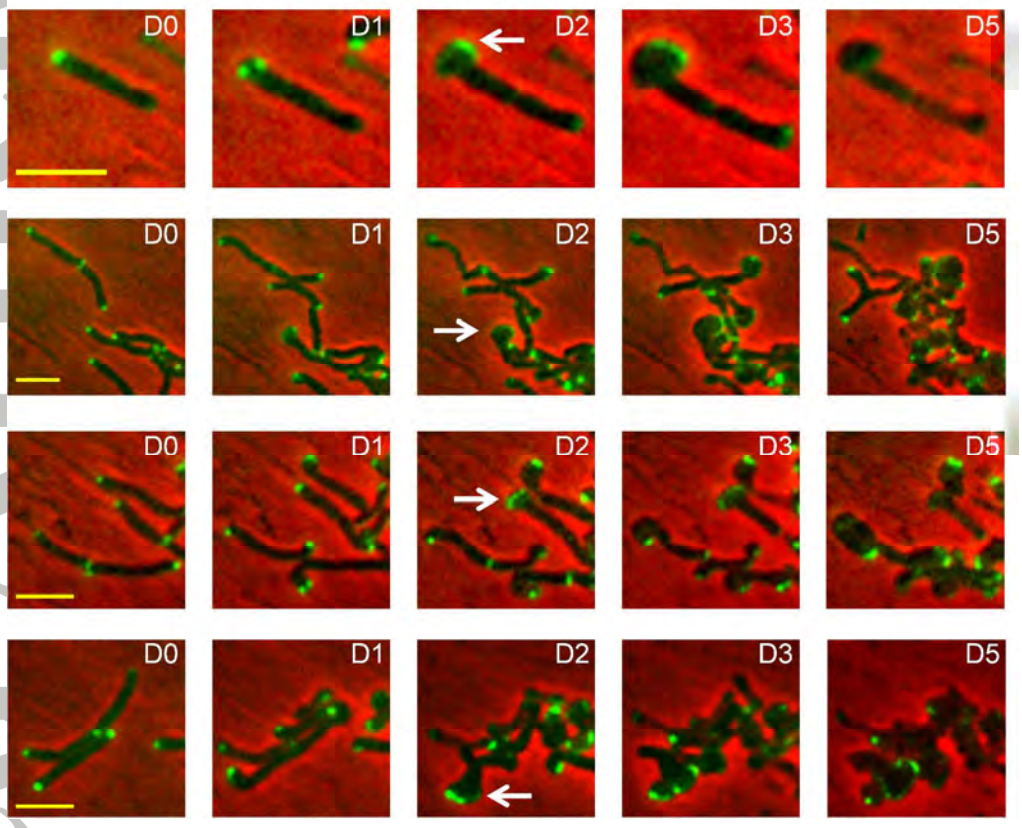

Figure 6:

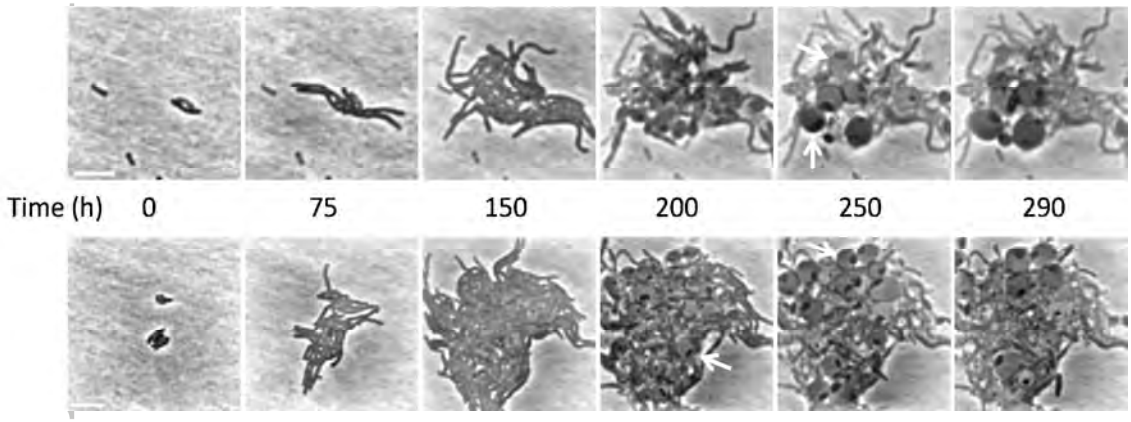

Figure 7.

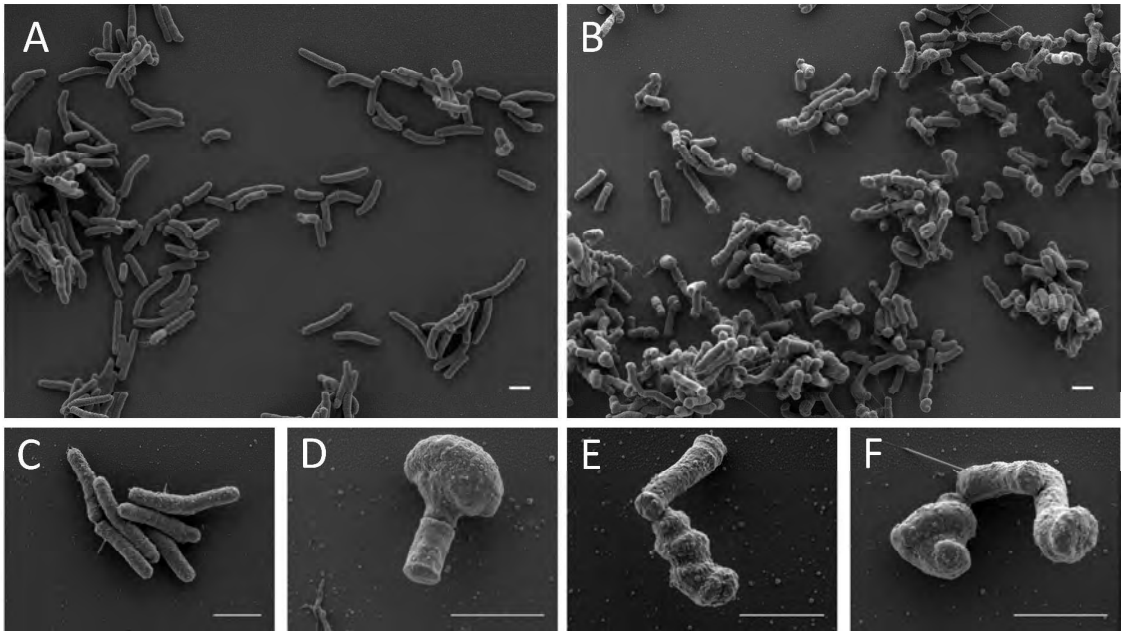

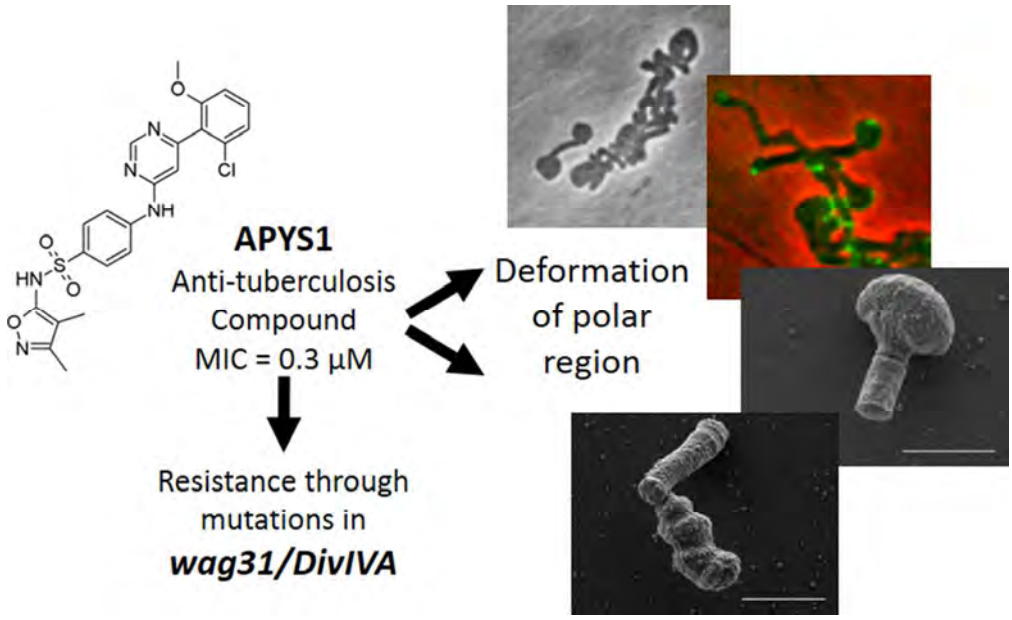
APYS1
Anti-tuberculosis
Compound
MIC = 0.3 µM
Resistance through
mutations in
wag31/DivIVA
Deformation
of polar
region